(14) G. F. Kokoszka, presented at the XVIth International Conference on Coordination Chemistry, Dublin, Ireland, Aug 1974; see paper 2.22a.
(15) S. J. Gruber, C. M. Harris, E. Kokot, S. L. Lenzer, T. N. Lockyer, and E. Sinn, *Aust. J. Chem.*, **20**, 2403 (1967).
(16) W. R. Busing and H. A. Levy, *Acta Crystallogr.*, **22**, 457 (1967).
(17) P. W. R. Corfield, R. J. Doedens, and J. A. Ibers, *Inorg. Chem.*, **6**, 197 (1967).
(18) For a discussion of the programs used, see E. D. Estes and D. J. Hodgson, *Inorg. Chem.*, **12**, 2932 (1973).
(19) D. T. Cromer and J. T. Waber, *Acta Crystallogr.*, **18**, 104 (1965).
(20) J. A. Ibers, "International Tables for X-Ray Crystallography", Vol. III, Kynoch Press, Birmingham, England, Table 3.3.1A.
(21) R. F. Stewart, E. R. Davidson, and W. T. Simpson, *J. Chem. Phys.*, **42**, 3175 (1965).
(22) J. A. Ibers and W. C. Hamilton, *Acta Crystallogr.*, **17**, 781 (1964).
(23) D. T. Cromer and D. Liberman, *J. Chem. Phys.*, **53**, 1891 (1970).
(24) D. T. Cromer, *Acta Crystallogr.*, **18**, 17 (1965).
(25) M. R. Churchill, *Inorg. Chem.*, **12**, 1213 (1973).
(26) D. L. Lewis and D. J. Hodgson, *Inorg. Chem.*, **13**, 143 (1974).
(27) Supplementary material.
(28) D. J. Hodgson and J. A. Ibers, *Inorg. Chem.*, **8**, 1282 (1969).
(29) B. J. Hathaway and D. E. Billing, *Coord. Chem. Rev.*, **5**, 158 (1970).
(30) W. H. Watson and D. R. Johnson, *J. Coord. Chem.*, **1**, 145 (1971).
(31) M. R. Kidd and W. H. Watson, *Inorg. Chem.*, **8**, 1886 (1969).
(32) M. Kato, H. B. Jonassen, and J. C. Fanning, *Chem. Rev.*, **64**, 99 (1964).
(33) R. J. Williams, W. H. Watson, and A. C. Larson, reported at the American Crystallographic Association Winter Meeting, Albuquerque, N.M., April 1972.
(34) D. R. Johnson and W. H. Watson, *Inorg. Chem.*, **10**, 1281 (1971).
(35) E. D. Estes, W. E. Estes, W. E. Hatfield, and D. J. Hodgson, *Inorg. Chem.*, **14**, 106 (1975).
(36) E. D. Estes and D. J. Hodgson, *J. Chem. Soc., Dalton Trans.*, 1168 (1975).
(37) D. Ülkü, B. P. Huddle, and J. C. Morrow, *Acta Crystallogr., Sect. B*, **27**, 432 (1971).
(38) V. F. Duckworth and N. C. Stephenson, *Acta Crystallogr., Sect. B*, **25**, 1975 (1969).
(39) D. H. Svedung, *Acta Chem. Scand.*, **23**, 2865 (1969).
(40) W. E. Hatfield and E. R. Jones, Jr., *Inorg. Chem.*, **9**, 1502 (1970).
(41) K. N. Raymond, D. W. Meek, and J. A. Ibers, *Inorg. Chem.*, **7**, 1111 (1968).
(42) L. Pauling, "The Nature of the Chemical Bond", 3rd ed, Cornell University Press, Ithaca, N.Y., 1960.
(43) A. Bondi, *J. Phys. Chem.*, **68**, 441 (1964).
(44) W. C. Hamilton and J. A. Ibers, "Hydrogen Bonding in Solids", W. A. Benjamin, New York, N.Y., 1968, p 116.
(45) J. T. Veal and D. J. Hodgson, *Inorg. Chem.*, **11**, 597 (1972).

Contribution from the Department of Polymer Chemistry, Waseda University, Tokyo 160, Japan

Formation and Decomposition of the Oxygen Complex of Ferroprotoporphyrin Bound to the Water-Soluble Polymer Ligand in Aqueous Solution

EISHUN TSUCHIDA,* KENJI HONDA, and HIROSHI SATA

Received January 21, 1975 AIC500498

The complexes formed between iron protoporphyrins (hemes) and partially quaternized poly(4-vinylpyridines) (QPVP's) were analyzed by spectrometry. The coordination number of the axial site of heme iron was determined to be near 1.0 so that the resulting major complexes were five-coordinate pyridine hemichromes or hemochromes. The equilibrium constants of ferri- and ferroprotoporphyrins were 2.60×10^2 and 2.77×10^4 M, respectively, and polymer-bound complexes were more stable than the corresponding monomeric analogues. The kinetics of reactions of the QPVP-bound ferroprotoporphyrins with molecular oxygen have been studied as a function of additives such as salt, surface-active agent, and polyelectrolyte. On the basis of the analytical results, it was confirmed that the resulting oxygen complex was a binuclear complex which may be formed successively via a mononuclear complex. The rate of decomposition of an oxygenated ferroprotoporphyrin decreased as a result of binding it to the polymeric ligand. The oxygen complex was consequently found to exist as a stable intermediate even in aqueous solution at room temperature.

Introduction

After Pfeiffer and Tsumaki[1] found that a cobalt–salcomin complex can bind molecular oxygen reversibly in crystalline form, many investigators have been interested in the studies on a reversible oxygen complex. Various types of oxygen complexes of iron, cobalt, and other metals were synthesized. Corwin and his co-workers[2] investigated the interaction between protein-free protoheme and dioxygen in solution and pointed out that the ferrous ion of heme is rapidly oxidized without formation of a detectable oxygen complex in water-containing solution. Calvin[3] reported the results of the reversible oxygen uptake of various cobalt–salcomin complexes in the solid state. Wang[4] and Hatano[5] synthesized a polymer-bound imidazole hemochrome as a model compound of hemoglobin and recognized the polymer effect on retardation of irreversible oxidation. Recently Collman,[6] Baldwin,[7] and Traylor[8] have succeeded in the synthesis of some interesting ferrous complexes which can bind dioxygen reversibly in solution at room temperature. Furthermore, Ibers,[9] Basolo,[10] and Walker[11] have studied the kinetics and thermodynamics of reversible oxygenation of cobalt(II) porphyrins in nonaqueous medium.

However, although many substantial studies have been developed on reversible oxygenation in solution, the study of the formation of an oxygen complex in an aqueous medium near room temperature has not satisfactorily been carried out yet. In this work, we try to stabilize an oxygen complex in a mixture of water and dimethylformamide at room temperature by binding ferroprotoporphyrin to the water-soluble polymeric ligand.

Experimental Section

Materials. Partially quaternized poly(4-vinylpyridine) was prepared according to the following method. Poly(4-vinylpyridine) (8.42 g) was dissolved in 150 ml of methanol and benzyl chloride (10.1 g) was dissolved in 50 ml of methanol. The polymer solution was charged into a four-necked round-bottom flask fitted with a dropping funnel and the benzyl chloride solution was dropped into the former solution from the dropping funnel. Stirred for 12 hr at 60°C, the solution was then condensed up to about 50 ml by evaporation and poured into 1000 ml of ethyl ether. The quaternized poly(4-vinylpyridine) obtained was dissolved in methanol and the solution was poured into ethyl ether. The precipitates were dried in vacuo. The degree of quaternization was determined to be 23.1% by the Volhard method.

Ferriprotoporphyrin chloride (chlorohemin) was extracted from blood by the Willstatter method.[12] Special grade commercial reagents of sodium hydrosulfite ($Na_2S_2O_4$) and sodium lauryl sulfate (NaLS) were used without purification. Distilled water was used through ion-exchange resin before use and the relative resistance of the water was above 10^6 Ω-cm.

Reduction and Oxygenation. Chlorohemin was reduced with $Na_2S_2O_4$ under the following conditions: [chlorohemin] = 2.0×10^{-5} M, [$Na_2S_2O_4$] = 2.0×10^{-3} M, [QPVP] = 2.0×10^{-2} M (a pyridine unit), in DMF–H_2O (1:4) at room temperature under a N_2 atmosphere. The reduction proceeded rapidly under the above conditions with a spectral change in the Soret band from 397 nm (due to a pyridine–hemin complex) to 422 nm (due to a pyridine–heme

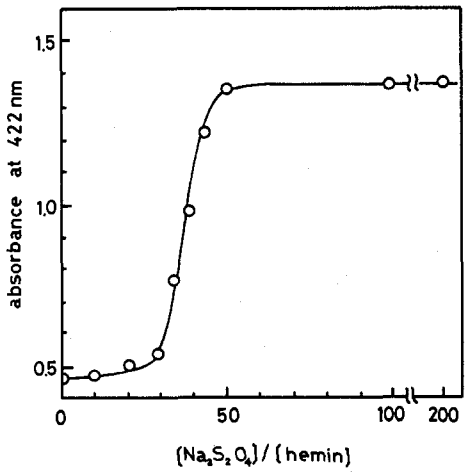

Figure 1. Relationship between the absorbance at 422 nm of the reduced ferrous complex and the molar ratio of $[Na_2S_2O_4]$/[hemin] in the reduction of chlorohemin; [hemin] = 1.0×10^{-5} M, [QPVP] = 1.0×10^{-2} M, in H_2O–DMF (8:2).

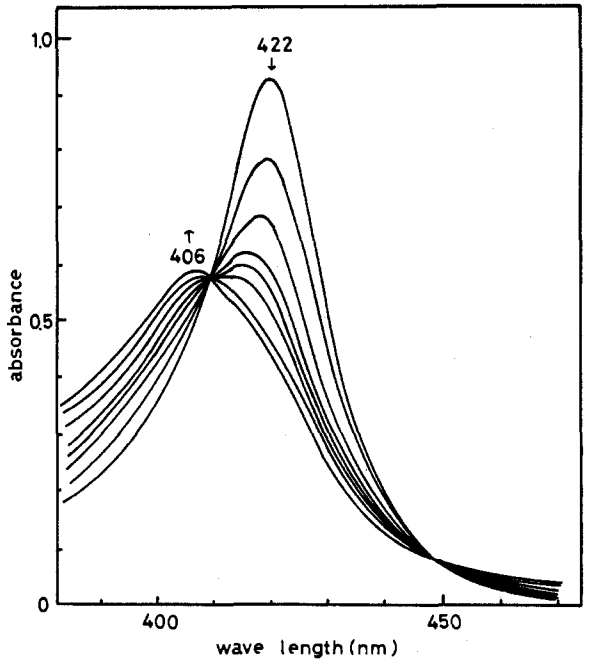

Figure 2. Spectral changes with time in oxygenation detected by use of a rapid-scan analyzer; [heme] = 1.0×10^{-5} M, [QPVP] = 1.0×10^{-2} M, in H_2O–DMF (8:2) at 25°C.

complex).[13] When the concentration of sodium dithionite added was equivalent to or 10 times as high as that of hemin, the absorption band at 422 nm characteristic of the reduced hemochrome could scarcely be observed. The absorbance at 422 nm became large when the molar ratio of sodium dithionite to hemin was above 30–40, as shown in Figure 1. It is thus preferable to make the concentration of sodium dithionite about 10^2 times as high as that of the hemin used.

After a 20% (volume) DMF-containing aqueous solution of the QPVP–heme complex had been mixed with oxygen-saturated water, spectral changes with time in the visible region were checked under oxygen. The absorbance at 422 nm gradually decreased with increasing absorbance at 406 nm (see Figure 2). The absorption band at 406 nm could hardly shift back to the absorption band at 422 nm by degassing the solution. However, the band at 406 nm is clearly distinguishable from the band at 397 nm due to the oxidized complex.

The first-order rate constant of irreversible oxidation of an oxygenated hemochrome was determined from the slope of a plot of log $|A_t - A_\infty|$ vs. time for the decrease with time in absorbance at 406 nm (see Figure 3). Half-life periods of the decay of the absorption band at 406 nm were used as the lifetime of the oxygen complexes. Visible spectra were recorded on a Shimadzu MPS-50L spectrophotometer and rapid reactions were detected by use of a rapid-scanning spectrophotometric analyzer (Union high-sense spectrophotometer, RA-1300).

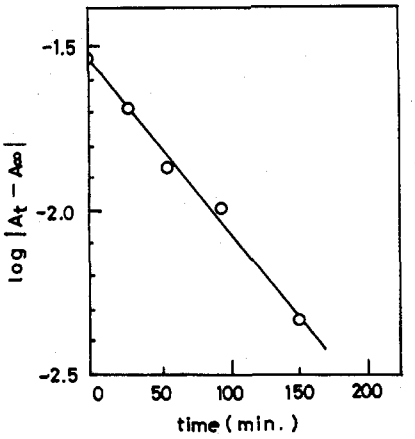

Figure 3. Determination of rate constant of the irreversible oxidation; [heme] = 1.0×10^{-5} M, [QPVP] = 1.0×10^{-2} M (Q % = 23.1, $\overline{Pn}$ = 49), [PMAA] = 2.3×10^{-3} M ($\overline{Pn}$ = 200), in H_2O–DMF (8:2), at 25°C.

Measurement of Magnetic Susceptibility. Powdery samples used for measuring magnetic susceptibilities were prepared by the following method. QPVP-bound hemichromes were prepared under the following conditions: chlorohemin (65 mg) and QPVP (69 mg) were dissolved in 40 ml of 0.02 M sodium carbonate buffer solution (pH 12) and the solution was stirred at room temperature and then evaporated under reduced pressure to form a black-brown powder. When QPVP-bound hemochromes were prepared, 400 mg of $Na_2S_2O_4$ was added to the chlorohemin solution at the same time. Magnetic susceptibilities were measured by the Faraday method.[14]

Results

Coordination of QPVP to Ferri- and Ferroprotoporphyrins. Visible spectra of the complex formation between ferri- and ferroprotoporphyrins and pyridine residues of the QPVP were measured in order to analyze the complexation quantitatively.[15] Mathematical relations useful in determining the equilibrium constant of eq 1 from the absorbance of an equilibrium mixture

$$P_M + nB \rightleftharpoons P_M\text{-}B_n \tag{1}$$

at chosen wavelength are

$$K = \frac{[P_M\text{-}B_n]}{[P_M][B]^n} = R\frac{1}{[B]^n} \tag{2}$$

$$R = X/(A - X) \tag{3}$$

$$A = D_c - D_u \tag{4}$$

$$X = D_m - D_u \tag{5}$$

If $[B] >> [P_M]$

$$\frac{1}{X} = \frac{1}{KA}\frac{1}{[B]^n} + \frac{1}{A} \tag{6}$$

where P_M is a base-free metalloporphyrin, B is an axial base of metalloporphyrin, P_M–B_n is a base-complexed metalloporphyrin, and K is the equilibrium constant for reaction 1. A, X, and R are defined by eq 3–5, respectively, where D_m is the absorbance of an equilibrium mixture at some given total metalloporphyrin concentration, and D_u and D_c are the absorbances which the total metalloporphyrin concentration would exhibit, if complexing were zero or complete, respectively.

The wavelengths useful in determining the equilibrium constant were 397 nm for ferriprotoporphyrin and 422 nm for ferroprotoporphyrin, respectively. Figure 4 shows the plots of the absorbances at 397 and 422 nm against the logarithmic

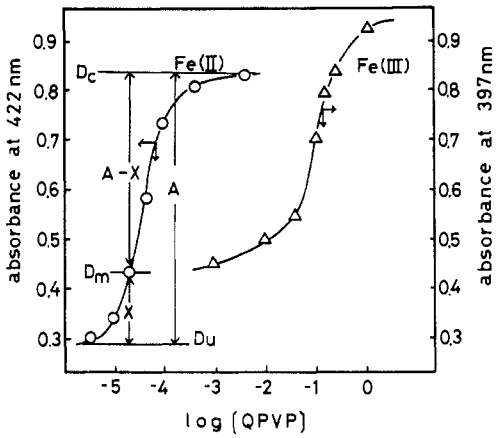

Figure 4. Changes in absorbance of the characteristic absorption bands in the complexation of ferri- and ferroprotoporphyrins with QPVP; [hemin] = 1.0×10^{-5} *M*, in H_2O-DMF (8:2), at 25°C.

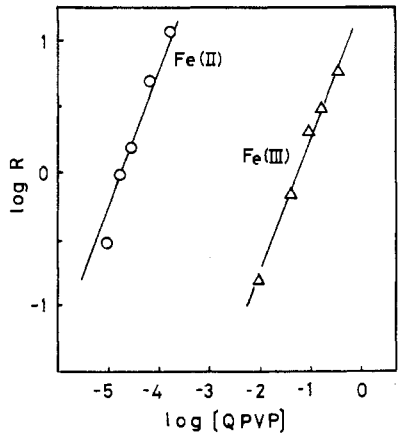

Figure 5. Determination of the coordination number of the axial ligand in the complexation of ferri- and ferroprotoporphyrins with QPVP.

Table I. Complex Formation between QPVP (or Pyridine) and Iron Protoporphyrin IX[a]

Metal ion	Axial ligand	Absorption λ_{max}, nm	$\tilde{n}$	K, M^{-1}	$10^6 \chi_M$, emu
Fe^{3+}	QPVP	397	1.30	2.60×10^2	13 000 ($s = 4.7/2$)
	Pyridine		1.02	3.72×10	12 700 ($s = 4.6/2$)
Fe^{2+}	QPVP	422	1.25	2.77×10^4	9 800 ($s = 3.9/2$)
	Pyridine		1.11	2.22×10^2	

[a] Conditions: [hemin] = 1.0×10^{-5} *M*, [ligand] = 10^0-10^{-5} *M*, in H_2O-DMF (9:1), at 25°C.

value of the concentration of pyridine unit of QPVP used. In Figure 5 the values of log *R* were plotted against the logarithmic values of concentration of the pyridine unit of QPVP. The coordination number ($\tilde{n}$) of the axial ligand was calculated from the slope of the straight line in this figure. The resultant values of $\tilde{n}$ were nearly equal to 1.0 for both the pyridine hemichrome and hemochrome.

If $\tilde{n}$ were unity in eq 6, the equilibrium constant can be determined by a plot of $1/X$ against $1/[B]$. In Figure 6, $1/X$ was plotted against the reciprocal of concentration of the pyridine unit of QPVP. The equilibrium constants calculated from the results of this experiment are presented in Table I. The corresponding equilibrium constants of the complexation between iron protoporphyrins and monomeric pyridine were

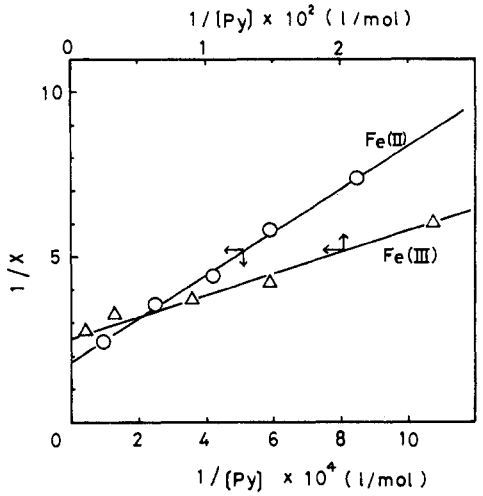

Figure 6. Determination of the equilibrium constant of the complexes of ferri- and ferroprotoporphyrins with QPVP.

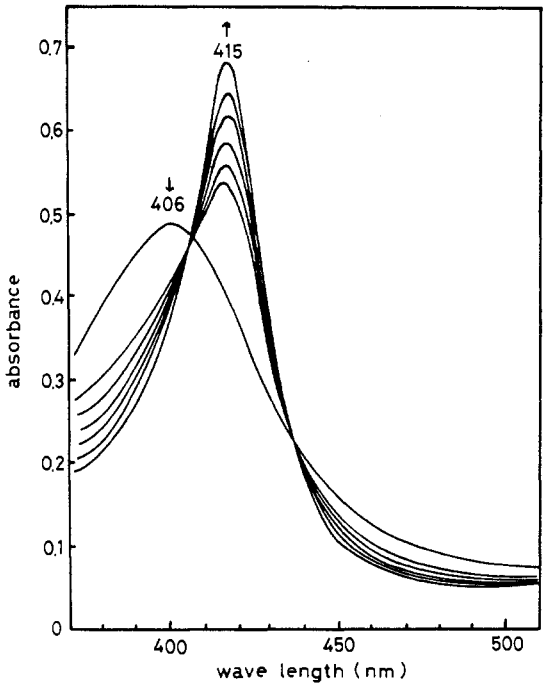

Figure 7. Spectral changes during the ligand-exchange reaction of the oxygen complex with carbon monoxide; [heme] = 1.0×10^{-5} *M*, [QPVP] = 1.0×10^{-2} *M*, [PMAA] = 2.3×10^{-2} *M*, in H_2O-DMF (8:2), at 25°C.

also determined. For both ferric and ferrous complexes, the equilibrium constants of the polymer system were much larger than those of the monomer system.

Formation of the Oxygen Complex of Ferroprotoporphyrin. The QPVP-bound hemichrome was reduced with sodium dithionite completely to form QPVP-bound hemochrome, which was then exposed to dioxygen in aqueous DMF at room temperature. Figure 2 shows the spectral changes with time of oxygenation which were detected on a rapid-scanning spectrophotometer. The absorption band which appeared at 406 nm after bubbling oxygen could hardly shift back to 422 nm by degassing the aqueous solution in vacuo. However, the band at 406 nm is distinguishable from the band at 397 nm characteristic of the oxidized pyridine hemichrome. It was found that the band at 406 nm shifted to 415 nm when carbon monoxide was bubbled into the solution containing the complex of 406 nm, as Figure 7 shows. When the pyridine hemichrome was exposed to carbon monoxide, the absorption maximum at 397 nm did not change. On the other hand, when the

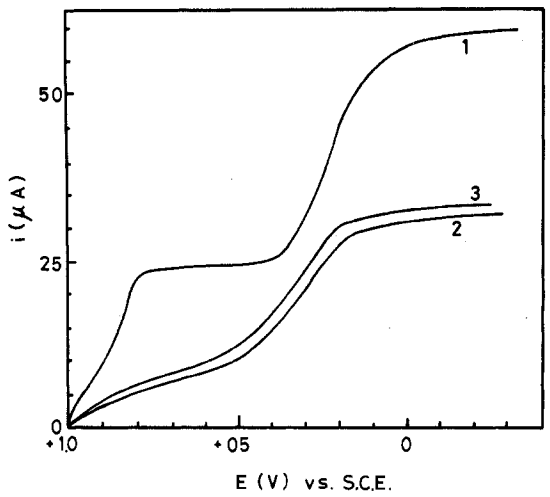

Figure 8. Polarogram of sodium dithionite in an aqueous solution: (1) $[Na_2S_2O_4] = 1.0 \times 10^{-2}$ *M*; (2) solution after bubbling O_2; (3) oxygen-saturated aqueous solution.

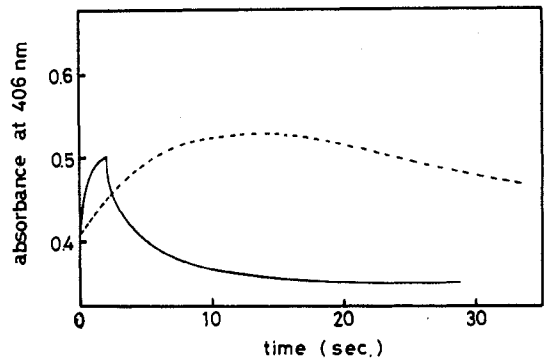

Figure 9. Decay of the absorbance at 406 nm due to the oxygen complex during the reaction of heme with dioxygen in an aqueous medium: ——, pyridine; - - - - -, QPVP.

pyridine hemochrome was exposed to carbon monoxide, the absorption maximum changed from 422 to 415 nm. Therefore, the band at 415 nm appears to be assignable to CO-bonded pyridine hemochrome. It is thus considered that the valence of heme iron still remains at the divalent state after exposure to dioxygen.

It was found by polarography that a large excess of sodium dithionite was completely oxidized by bubbling oxygen in the oxygenation of the hemochrome. The oxidation wave of sodium dithionite was observed in the vicinity of 0.5 V[16] on the polarogram of nitrogen-saturated aqueous solution containing sodium dithionite. When oxygen was bubbled into the solution for 15 min, this oxidation wave disappeared and the resulting polarogram was very similar to that of oxygen-saturated aqueous solution which did not contain sodium dithionite (see Figure 8). Therefore, the spectral change due to the ligand exchange with carbon monoxide may not be caused by the excess of sodium dithionite.

It is concluded that the band at 406 nm can be assigned to oxygenated pyridine hemochrome. Figure 9 shows the changes with time in absorbance at 406 nm during the reaction with dioxygen in aqueous DMF. When QPVP was used as the axial ligand instead of monomeric pyridine, the decay of the absorbance was slow.

Hydrophobic Environmental Effect on Autoxidation of the Oxygen Complex. When sodium chloride was added to the aqueous solution containing the QPVP-bound hemochrome, the reduced viscosity of the polymer solution decreased with increasing concentration of sodium chloride added. The rate constant of irreversible oxidation of heme iron(II) decreased with a decrease in the reduced viscosity of the polymer solution (see Figure 10(a)). It is well-known that a polyelectrolyte shrinks with the concentration of salt added.[17] In fact, the decrease in reduced viscosity of QPVP indicates the salt-induced shrinkage of polymer chains. It was thus clearly observed that the irreversible oxidation could be retarded as a result of inclusion of heme into the compactly shrunken polymer chains.

Figure 10(b) shows the similar effect of a surface-active agent on the kinetics of oxygenation of monomeric pyridine hemochrome. The rate constant of the irreversible oxidation decreased in the vicinity of the critical micelle concentration (8.0×10^{-3} *M*) of sodium lauryl sulfate. On the basis of the spectral analysis, it was found that the pyridine hemochrome was included in the globular micelle of sodium lauryl sulfate. When the Soret band of the pyridine hemochrome was checked as a function of the concentration of sodium lauryl sulfate, the absorption maximum gradually shifted to the red band region with increasing concentration of sodium lauryl sulfate and the absorbance became much larger in the vicinity of the critical micelle concentration. This may be due to inclusion of the pyridine hemochrome into the hydrophobic globular micelle of sodium lauryl sulfate.

The similar results were obtained by use of poly(methacrylic acid) (PMAA) and poly(styrenesulfonic acid) (PSS) as an additive, as Figure 10(c) indicates. When PMAA was added to the solution containing the QPVP-bound hemochrome, the reduced viscosity of the mixture continued to decrease until

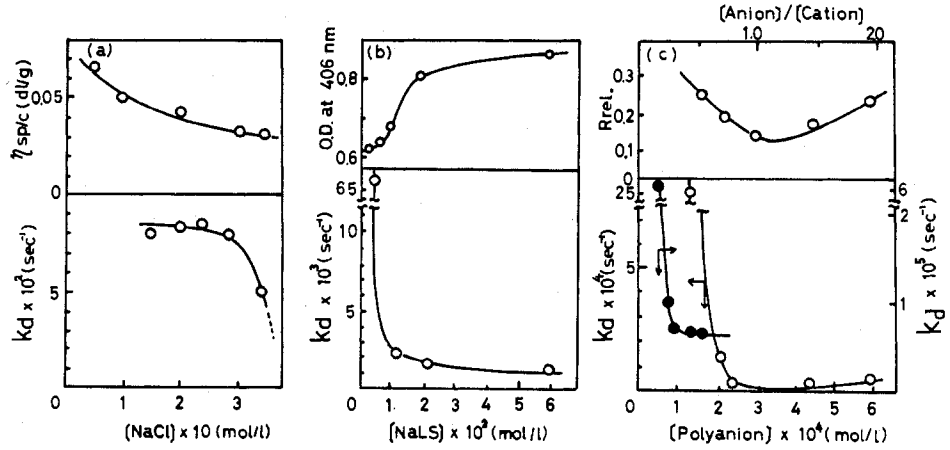

Figure 10. Effect of additives on kinetics of the irreversible oxidation in the (a) salt system, (b) micelle system, and (c) polyion complex system: ○, QPVP-PMAA; ●, QPVP-NaSS. [Heme] = 1.0×10^{-5} *M*, [py] = 1.0×10^{-2} *M*, [QPVP] = 10^{-4}-10^{-2} *M*, in H_2O-DMF (8:2), at 25°C. $R_{rel} = [\eta_{sp}/c(\text{QPVP} + \text{PMAA})]/[\eta_{sp}/c(\text{QPVP}) + \eta_{sp}/c(\text{PMAA})]$.

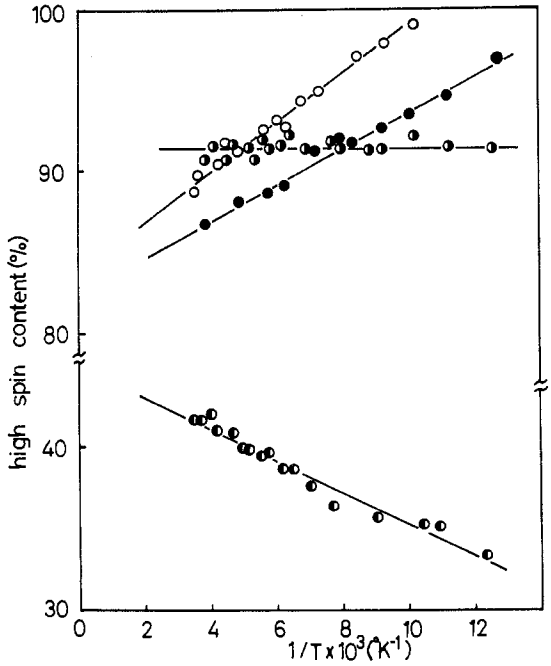

Figure 11. Relationship between the molar composition of the high-spin complex and inverse temperature: ●, Fe^{III}-py; ○, Fe^{III}-PVP; ◐, Fe^{III}-QPVP; ◑, Fe^{II}-QPVP.

the molar ratio of the quaternized pyridinium group of QPVP against the carboxylic group of PMAA became unity. At higher levels of the PMAA concentration, the solution viscosity became larger. The above results indicate that QPVP can bind PMAA through electrostatic interaction to form a polyion complex. The rate constant of the irreversible oxidation also continued to decrease with decreasing reduced viscosity until the molar ratio of the cationic site of QPVP to the anionic site of PMAA became about 1.0 and the rate constant became approximately constant above this concentration of PMAA. QPVP can also interact with PSS through electrostatic force to form a polyion complex similar in structure to that of the polyion complex between QPVP and PMAA. The rate constant of irreversible oxidation of this system also decreased with an increase in the concentration of PSS added (see Figure 10(c)).

Discussion

Coordination Structures of QPVP-Bound Iron Protoporphyrins. On the basis of the results represented in Table I, it is clear that the fifth coordination site of heme iron is occupied by the pyridine unit of QPVP. Most of the coordination numbers presented in Table I are intermediate between 1.0 and 2.0 so that the six-coordinate complex, whose axial sites of heme iron are both occupied by two pyridine units of QPVP, probably coexists with the five-coordinate complex. The magnetic susceptibilities presented in Table I also indicate that a high-spin complex coexists with a low-spin complex, because the molar magnetic susceptibilities of the pyridine hemichromes were intermediate between the calculated value of molar magnetic susceptibility of the high-spin complex (the five-coordinate complex) and that of the low-spin complex (the six-coordinate complex). On the basis of the result of temperature dependence of the magnetic susceptibility, as Figure 11 indicates, it was found that the high-spin complex and the low-spin complex were at spin equilibrium. On the other hand, the magnetic susceptibility of the hemochrome was independent of inverse temperature, which was nearly equal to the calculated value of the high-spin complex. Therefore, in case of the pyridine-bound hemochrome, the six-coordinate pyridine hemochrome may scarcely coexist with the five-coordinate one.

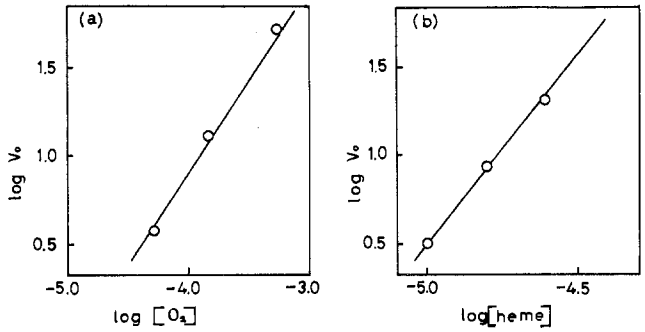

Figure 12. Kinetic orders of oxygenation rate with respect to heme iron and dioxygen: (a) dependence upon heme iron concentration; (b) dependence upon dioxygen concentration. [Heme] = 2.0×10^{-5} *M*, for part a, $[O_2]_0 = 1.5 \times 10^{-5}$ *M*, for part b, [QPVP]/[heme] = 10^3, in H_2O-DMF (8:2), at 25°C.

However, the result of the magnetic measurement is not always in agreement with the result of the spectrophotometrical analysis, as Table I indicates. The details are now under investigation.

On the basis of the results of the equilibrium constants, it was found that the polymer-bound metalloporphyrins were much more stable than the monomeric analogues. In general, polymer-bound metal complexes are more stable than monomeric analogues on account of accumulation of coordination groups in the polymer domain.

Mechanism of Formation of the Oxygen Complex. The absorption band at 406 nm can be assigned to the oxygenated pyridine hemochrome, as mentioned above. This intermediate immediately decomposed when the axial ligand of heme iron was monomeric pyridine. On the other hand, it was relatively stable when the polymer ligand was used, as Figure 9 shows. The oxygen complex was always detected as the intermediate of the autoxidation. It is generally believed from the mechanism of autoxidation in previous studies[9,10] that a mononuclear oxygen complex is formed in the first step and then dimerizes to form a binuclear oxygen complex, which immediately decomposes by itself with formation of an oxidized complex. It is also well-known that hemoglobin forms a stable mononuclear oxygen complex without formation of a binuclear oxygen complex owing to steric factors of apoprotein.[4] We have studied the kinetics of oxygenation and autoxidation of polymer-bound ferroprotoporphyrins in order to clarify the mechanism of the reactions.

Kinetic orders with respect to heme iron and dioxygen were determined from the rate of oxygenation of the QPVP-bound hemochrome. As Figure 12 shows, the rate was proportional to second order in heme iron concentration and first order in dioxygen concentration. Then, the rate of oxygenation of the QPVP-bound hemochrome is presented by

$$V = k[Fe^{II}]^{2.0}[O_2]^{1.0} \tag{7}$$

This result indicates that two hemes and one dioxygen participate in the oxygenation; that is, the resulting oxygen complex is a binuclear complex. The bimolecular mechanism expressed by eq 8 may be plausible for the oxygenation and

$$Fe^{II} + O_2 \overset{k_1}{\rightleftharpoons} Fe^{II}\text{-}O_2 \xrightarrow[Fe^{II}]{k_2} Fe^{III}\text{-}O_2^{2-}\text{-}Fe^{III} \xrightarrow{k_3} 2Fe^{III} \tag{8}$$

autoxidation. If the rate of the second step is lower than that of the first step, eq 7 can be explained reasonably. In case of monomeric complexes, the rate constant of k_2 is in general much higher than the rate constant of k_1. On the other hand, in case of polymer-bound hemochromes, k_1 is higher than k_2 owing to the steric hindrance of polymer chains, so that the second step in eq 8 may be the rate-determining step in this case. The amount of dioxygen absorbed at equilibrium was

Table II. Stability of the Oxygenated Pyridine Ferroprotoporphyrins

Axial ligand	Additive	Lifetime,[a] sec	Min rate const of oxidn, sec^{-1}
Pyridine	None	1.0	
	NaLS	30	2.12×10^{-3}
QPVP	NaCl	30	5.07×10^{-2}
	PMAA	3000	2.30×10^{-5}
	NaSS	9600	8.90×10^{-6}

[a] The lifetime is the half-life period of the absorption band at 406 nm (or 410 nm for the 9600-sec lifetime).

equal to half the initial amount of heme. It is also considered from this result that the binuclear oxygen complex is formed as the final product.

Stability of the Oxygen Complex in Aqueous Dimethylformamide. The electronic structure of the oxygen complex has been studied for various Co^{II}–O_2 adducts by the x-ray[18-20] and ESR[21-23] techniques and the following structures have been presented on the basis of the results: Co^{III}–O_2^{2-}–Co^{III} for a diamagnetic binuclear complex, Co^{III}–O_2^{-}–Co^{II} for a paramagnetic binuclear complex, and Co^{III}–O_2^{-} for a paramagnetic mononuclear complex. With respect to Fe^{II}–O_2 adducts, Weis[24] proposed the superoxo structure (Fe^{III}–O_2^{-}) for oxyhemoglobin. However, the oxygen complex of Fe^{II}–O_2 also should be expressed by the resonance form between the nonbond structure (Fe^{II}···O_2) and the dative structure (Fe^{III}–O_2^{-}). The binuclear oxygen complex may be expressed as {Fe^{II}–O_2–Fe^{II} ↔ Fe^{III}–O_2^{2-}–Fe^{III}}. The binuclear oxygen complex decomposes rapidly with the dissociation of the ion pair of the dative form especially in polar media such as water. As the result, the oxygen complex has not been detected as a stable form in a medium containing a large amount of water. However, it is well-known that hemoglobin can form the stable oxygen complex in water at room temperature. Such a behavior of oxyhemoglobin is based on the following facts. (1) Formation of the binuclear oxygen complex is retarded owing to the steric effect of apoprotein so that the mononuclear complex exists as a stable form. (2) The dissociation of the ion pair of the oxygen complex is retarded by the hydrophobic cavity which is called the heme pocket. The stabilization of the oxygen complex of hemoglobin can be explained in terms of the steric effect and the hydrophobic environmental effect of apoprotein.

The present authors have tried to endow a synthetic model with the above-described functions of hemoglobin by substituting globin moieties for synthetic polymers. As already represented in Figure 10, if heme iron were included into a hydrophobic domain, the oxygen complex is to be stabilized. Although the polarity of solution in general becomes larger with increasing ionic strength, the dissociation of the ion pair of the oxygen complex was retarded with the ionic strength. The reason for such an apparently contrary result is that the polarity of the local field around heme becomes lower with the concentration of salt added, because the polymer chain of QPVP shrinks with increasing ion strength (see Figure 10(a) upper) so that heme is included in the hydrophobic microenvironment of the compactly shrunken polymer chains. Similar results of the micelle system and the polyion complex system can be explained by the same reason as described above. It is noticeable that, as poly(methacrylic acid) is a poorly dissociated electrolyte, the pH value of the aqueous solution scarcely decreased by adding poly(methacrylic acid). Therefore, the decomposition of oxygen complex caused by the acidic protons of poly(methacrylic acid) can be neglected. Table II presents the lifetimes of oxygen complexes and the minimum rate constants of the irreversible oxidation as functions of additives. It is suggested on the basis of the data that the lifetimes of oxygen complexes change with the dielectric constant of the local field around heme iron.

In addition, it should be noted that the rate constants of the oxidation did not depend at all upon the concentration of sodium dithionite used as a reductant. After the chemical environment of the heme-containing domain will have been quantitatively estimated by some methods, the details of such polymer effects on oxygenation will be further discussed.

Acknowledgment. The authors gratefully acknowledge support for this research by a grant-in-aid for scientific research from the Ministry of Education, Tokyo, Japan (No. 085203).

Registry No. Ferroprotoporphyrin, 14875-96-8; ferriprotoporphyrin chloride, 15489-47-1; ferroprotoporphyrin pyridine complex, 57474-03-0; ferriprotoporphyrin chloride pyridine complex, 51321-27-8; PVP, 100-43-6; NaLS, 151-21-3; PMAA, 25087-26-7; NaSS, 9080-79-9; NaCl, 7647-14-5.

References and Notes

(1) P. Pfeiffer, E. Breith, E. Lübbe, and T. Tsumaki, *Justus Liebigs Ann. Chem.*, **503**, 84 (1933).
(2) (a) A. H. Corwin and J. G. Erdman, *J. Am. Chem. Soc.*, **68**, 2473 (1946); (b) A. H. Corwin and Z. Reyes, *ibid.*, **78**, 2437 (1956); (c) A. H. Corwin and S. D. Bruck, *ibid.*, **80**, 4736 (1958).
(3) (a) M. Calvin, R. H. Bailes, and W. K. Wilmarth, *J. Am. Chem. Soc.*, **68**, 2254 (1946); (b) C. H. Barkelen and M. Calvin, *ibid.*, **68**, 2257 (1946); (c) R. H. Bailes and M. Calvin, *ibid.*, **69**, 1886 (1947).
(4) (a) J. H. Wang, A. Nakahara, and E. B. Fleischer, *J. Am. Chem. Soc.*, **80**, 1109 (1958); (b) J. H. Wang, *ibid.*, **80**, 3168 (1958); (c) J. H. Wang, *Acc. Chem. Res.*, **3**, 90 (1970).
(5) M. Hatano, *Kagaku Kogyo*, **18**, 926 (1965); *Kobunshi*, **13**, 292 (1964).
(6) (a) J. P. Collman and C. A. Reed, *J. Am. Chem. Soc.*, **95**, 2048 (1973); (b) J. P. Collman, R. R. Gagne, T. R. Harbert, J. C. Marchon, and C. A. Reed, *ibid.*, **95**, 7868 (1973); J. P. Collman, R. R. Gagne, C. A. Reed, T. R. Harbert, G. Lang, and W. T. Robinson, *ibid.*, **97**, 1427 (1975).
(7) (a) J. E. Baldwin and J. Huff, *J. Am. Chem. Soc.*, **96**, 5600 (1974); (b) J. Almog, J. E. Baldwin, R. L. Dyer, and M. Peters, *ibid.*, **97**, 226 (1975).
(8) C. K. Chang and T. G. Traylor, *J. Am. Chem. Soc.*, **96**, 5595 (1974).
(9) (a) H. C. Stynes and J. A. Ibers, *J. Am. Chem. Soc.*, **94**, 1559, 5125 (1972); (b) D. V. Stynes, H. C. Stynes, J. A. Ibers, and B. R. James, *ibid.*, **95**, 1142, 1796 (1973).
(10) (a) M. J. Carter, D. P. Rillema, and F. Basolo, *J. Am. Chem. Soc.*, **96**, 392 (1974); (b) D. L. Anderson, C. J. Weschler, and F. Basolo, *ibid.*, **96**, 5599 (1974).
(11) F. A. Walker, *J. Am. Chem. Soc.*, **95**, 1150, 1554 (1973).
(12) R. Willstätter, *Justus Liebigs Ann. Chem.*, **365**, 197 (1950).
(13) E. Tsuchida, K. Honda, and H. Sata, *Biopolymers*, **13**, 2147 (1974).
(14) E. Tsuchida, K. Honda, H. Hata, H. Suwa, and K. Kohn, *Chem. Lett.*, 761 (1975).
(15) J. R. Miller and G. D. Dorough, *J. Am. Chem. Soc.*, **74**, 3977 (1952).
(16) W. J. Lem and M. Wayman, *Can. J. Chem.*, **48**, 776 (1970).
(17) C. Tanford, "Physical Chemistry of Macromolecules", Wiley, New York, London, 1969, p 492.
(18) (a) R. E. Marsh and W. P. Shaefer, *Acta Crystallogr., Sect. B*, **24**, 246 (1968); (b) W. P. Shaefer and R. E. Marsh, *Acta Crystallogr.*, **21**, 735 (1966); (c) C. G. Cristoph, R. E. Marsh, and W. P. Shaefer, *Inorg. Chem.*, **8**, 291 (1969).
(19) M. Calligaris, G. Nardin, L. Randaccio, and A. Ripamonti, *J. Chem. Soc. A*, 1069 (1970).
(20) M. W. Terry, E. L. Amma, and L. Vaska, *J. Am. Chem. Soc.*, **94**, 653 (1972).
(21) (a) E. A. V. Ebsworth and J. A. Weil, *J. Phys. Chem.*, **63**, 1890 (1959); (b) J. A. Weil and J. K. Kinnaird, *ibid.*, **71**, 3341 (1967).
(22) B. M. Hoffman, D. L. Diemente, and F. Basolo, *J. Am. Chem. Soc.*, **92**, 61 (1970).
(23) G. N. Schrauzer and L. P. Lee, *J. Am. Chem. Soc.*, **92**, 1551 (1970).
(24) J. J. Weis, *Nature (London)*, **202**, 83 (1964).